Proceedings of Ninth World Conference on Earthquake Engineering
August 2-9, 1988, Tokyo-Kyoto, JAPAN (Vol.III)

4-3-15

UNDRAINED STRESS STRAIN BEHAVIOR OF SAND SUBJECTED TO EARTHQUAKE WAVE LOADING

Tej B.S. PRADHAN[1], Fumio TATSUOKA[2] and Yasuhiko SATO[3]

[1]Osaka Soil Test Laboratory, Nishi-ku, Osaka, Japan
[2]Formerly, Institute of Industrial Science, University of Tokyo
[2]Institute of Industrial Science, University of Tokyo,
[3]Minato-ku, Tokyo, Japan
[3]Research Institute of Nishimatsu Construction Co.,
Yamato-shi, Kanagawa, Japan

SUMMARY

Presented in this paper are a method for cyclic undrained simple shear testing on saturated sand and the results obtained by using irregular cyclic shear stresses. The results show that the relationships between the shear stress and the shear strain are extremely complicated and cannot be modelled by a simple constitutive relation. However, the relationships between the ratio of shear stress to the current effective pressure and the shear strain are of smooth elasto-plastic, strain-hardening hyperbolic-type one.

INTRODUCTION

For an earthquake response analysis of a liquefying saturated sand deposit, an appropriate constitutive relation of sand is required. While a great number of cyclic undrained tests on saturated sands have been performed by means of, for example, the triaxial apparatus, they were mostly stress-controlled and from the results it is rather difficult to examine in detail the stress-strain relationships of liquefying sand, especially at low effective pressure levels. Accurate stress-strain relationships obtained so far by means of strain-controlled tests are rather limited (for example, Refs 1 and 2).

Reported herein are the results of two strain-controlled cyclic undrained simple shear tests of loose and dense sand specimens. Based on them together with the result of one cyclic drained simple shear test, the stress-strain relationship of liquefying sand will be discussed.

TEST METHODS

The simple shear test is the most appropriate measure for simulating the behavior of a sand element in a level ground under earthquake loading. For this purpose, the torsional simple shear testing method using a hollow cylindrical specimen as shown in Fig.1 was employed (Ref.3). One of the advantages of this testing method is that all the three principal stresses can be defined. The simple shear deformation is that the shape and size of all the horizontal cross-sections of specimen are kept unchanged during shearing (i.e., $\dot{\varepsilon}_r=\dot{\varepsilon}_t=0$, see Fig.1). For undrained tests, this condition can be realized by the following three mechanical measures; (1) the constant specimen volume condition by making the saturated specimen undrained, (2) the constant height condition and (3) the constant volume condition of the water-saturated inner hollow.

The specimens were prepared by pluviating air-dried Toyoura sand (G_s=2.64,

U_c=1.46, D_{50}=0.16mm, no fines content, sub-angular to angular grain shape, e_{max}=0.977, e_{min}=0.605). After being saturated, they were anisotropically consolidated at the stress ratio σ'_r/σ'_a=0.40 to an effective mean principal stress $\sigma'_{m_c}=(\sigma'_{a_c}+2\sigma'_{r_c})/3$ of 1.0 kgf/cm^2. This stress ratio is very close to that under the one-dimensional compression.

Under the undrained condition, irregular cyclic shear stresses were applied at a constant shear strain rate $\dot{\gamma}_{at}$=0.1%/min (see Figs 2b and 4b). The time history of cyclic shear stresses used in the present study simulates only the sequences of reversing points and the relative largeness of pulses at reversing points in a recorded accelerogram. This is the horizontal N-S component of the earthquake

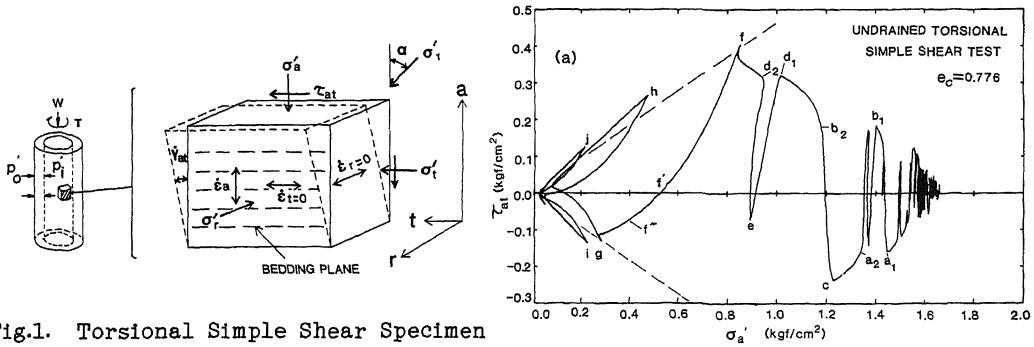

Fig.1. Torsional Simple Shear Specimen

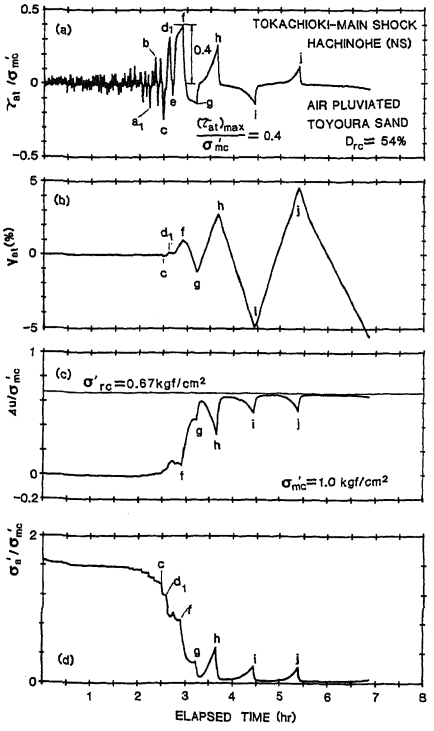

Fig.2. Time Histories of Measured Quantities for Loose Specimen

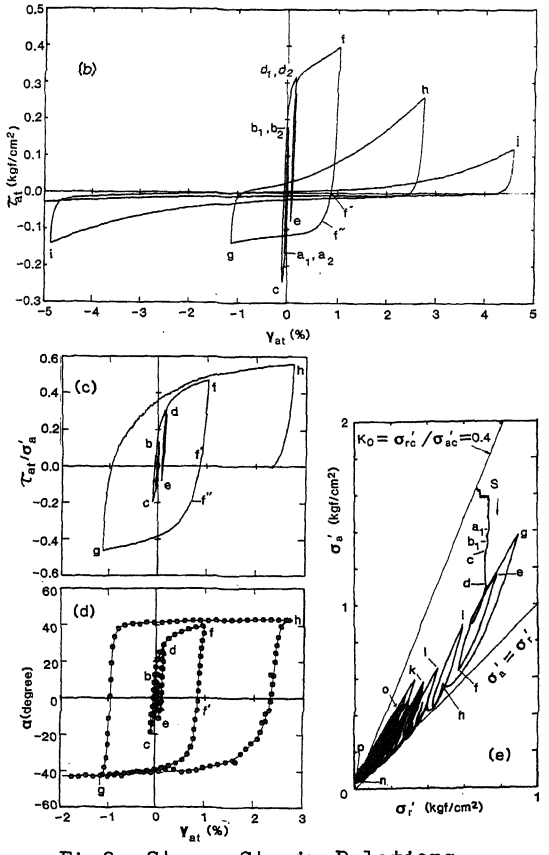

Fig.3. Stress-Strain Relations for Loose Specimen

motion recorded on the ground surface at Hachinohe during the major shock of the Tokachi-oki earthquake of 1968 (Magnitude=7.9, the epicentral distance=189 km, the maximum acceleration=235 gals). Consequently, the shape of the time history of cyclic shear stresses shown in Figs 2(a) and 4(a) is distorted in the direction of the horizontal coordinate of time from that of the original accelerogram ; i.e., against a constant shear strain rate in the present tests, in

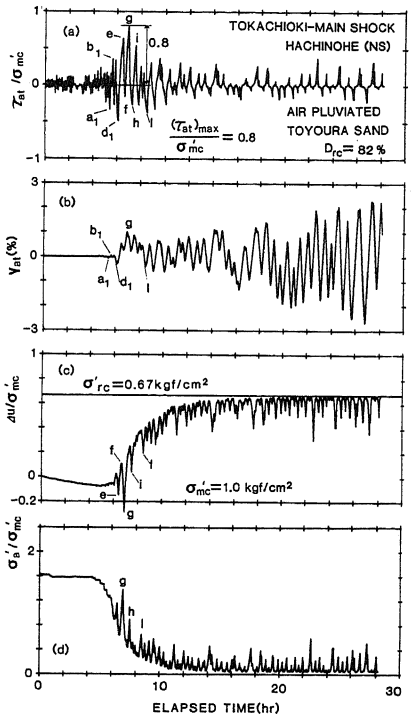

Fig.4(above).
Time Histories of Measured Quantities for Dense Specimen

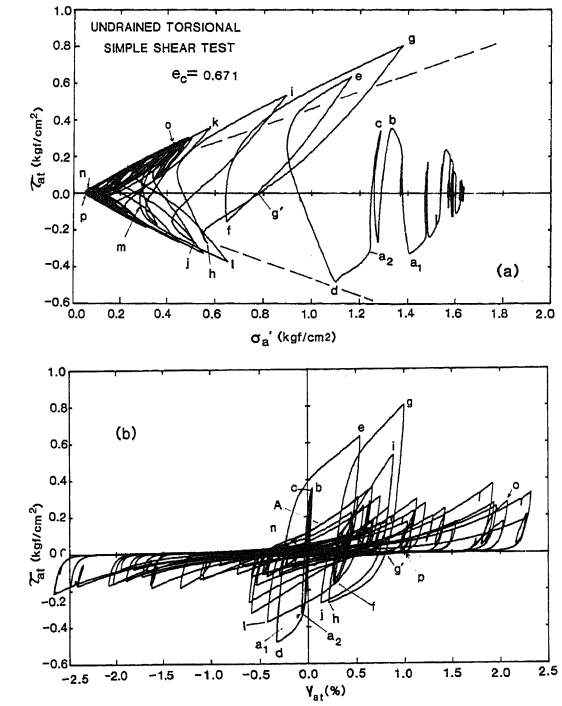

Fig.5(right).
Stress-strain Relations for Dense Specimen

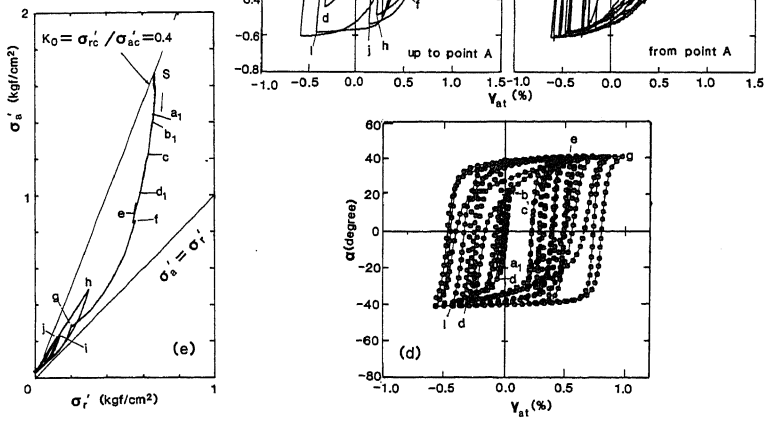

the field it is not constant, usually increasing in the process of liquefaction. This method can be justified for the purpose of simulating the stress-strain behavior of an soil element at a shallower deposit during an earthquake motion by the following reasons: (1) the time history of shear stresses on horizontal planes at shallower depths in the field is similar in shape to that of horizontal acceleration on the ground surface, and (2) the effect of shear strain rate on the stress-strain relations of clean sands as used in the present study is known to be very small.

For the purpose of very accurate measurements of stress values, especially at extremely low effective pressure levels, the following methods were found essential (Refs 2, 3, 4); (1) the measurements of both axial load and torque inside the triaxial cell, (2) the direct measurement of effective lateral pressures p'_o and p'_i by means of two differential pressure transducers (p'_o is the cell pressure minus the pore water pressure and p'_i is the inner hollow pressure minus the pore water pressure), (3) corrections of all stress components for membrane forces, and (4) tests at a constant and very slow shear strain rate. As to the term (4), it is to be noted that in usual stress-controlled tests, the strain rate becomes extremely large when approaching the liquefied condition and, therefore, accurate measurements of stresses become extremely difficult.

TEST RESULTS

Fig.2 shows the time histories of (a) the shear stress τ_{at} divided by σ'_{m_c}, (b) the shear strain γ_{at}, (c) the excess pore water pressure Δu, divided by σ'_{m_c}, and (d) the effective axial stress σ'_a divided by σ'_{m_c}, for a loose specimen. Fig.3 shows the stress-strain relations constructed from the data shown in Fig.2. Figs 4 and 5 are similar ones for a dense specimen. In these figures, stresses are defined at the mid-height of specimen. In Fig.5(c), for simplicity, the relations up to and after the point A are shown separately. In Figs 3(d) and 5(d), α means the angle of σ'_1-direction relative to the σ'_a-direction (the vertical direction). Further, in Figs 3(c), 3(d), 5(c) and 5(d), the data points have been plotted only before the values of τ_{at}/σ'_a and α become very unstable because of extremely low effective pressures. The following points may be seen from these figures.

(1) The relationships between τ_{at} and γ_{at} (Figs 3c and 5c) are extremely complicated, whereas the relationships between τ_{at}/σ'_a and γ_{at} are of smooth strain-hardening hyperbolic type one, which can be simulated by an appropriate elasto-plastic model.

(2) The decrease in σ'_a or increase in Δu is associated with the following two types of plastic shear deformation. The first type takes place during loading (i.e., τ_{at}/σ'_a increasing) when exceeding the previous maximum stress ratio τ_{at}/σ'_a in the current direction of shearing; i.e., for example, in Fig.3, from a_2 to c, from b_2 to d_1 and from d_2 to f, and in Fig.5, from a_2 to d. This type of plastic shear strain is the major cause for the build-up of Δu at smaller strains before the stress path exceeds the phase transformation line as shown by broken lines in Figs 3a and 5a; when the stress point is above the line, the specimen exhibits the cyclic mobility (the increase in the effective stress due to shear strain increment).

The second type of plastic shear strain occurs during unloading (i.e., τ_{at}/σ'_a decreasing) and during subsequent reloading in the other direction after having passed the neutral point (i.e., $\tau_{at}=0$). This type of plastic shear strain during unloading and reloading can be seen in Fig.3 from f to f' and from f' to f'', respectively, and in Fig.5, from g to g' and from g' to h, respectively. This type is the cause for the build-up of Δu at large strains after the cyclic mobility starts. This point can be confirmed in the results of cyclic drained simple shear test shown in Fig.6, since the change in Δu in an undrained test corresponds to the plastic volumetric strain increment dv_d induced by shear strain increment in a drained test.

The drained test was performed using also Toyoura sand by means of the same apparatus as used for the undrained tests [5]. The values of dv_d were obtained

as the measured total volumetric strain increment dv minus the volumetric strain increment dv_c due to the change in σ'_m. $d\gamma^p_{at}$ is the plastic shear strain increment obtained as the measured total shear strain increment $d\gamma_{at}$ minus the elastic component $d\gamma^e_{at}$. Fig.6(c) shows the so-called stress-dilatancy relation. It may be seen from Fig.6(c) that when the loading direction is reversed, the dilatancy rate changes discontinuously. For example, from i' to j, with $d\gamma^p_{at}>0$ the volume is increasing ($dv_d<0$), thus $-dv_d/d\gamma^p_{at}>0$ and $dv_d/|d\gamma^p_{at}|<0$. After reversing, from j to k', with $d\gamma^p_{at}<0$ the volume is decreasing ($dv_d>0$), thus $-dv_d/d\gamma^p_{at}>0$ and $dv_d/|d\gamma^p_{at}|>0$. Further, it may be noted that the rate of volume decrease (i.e.,

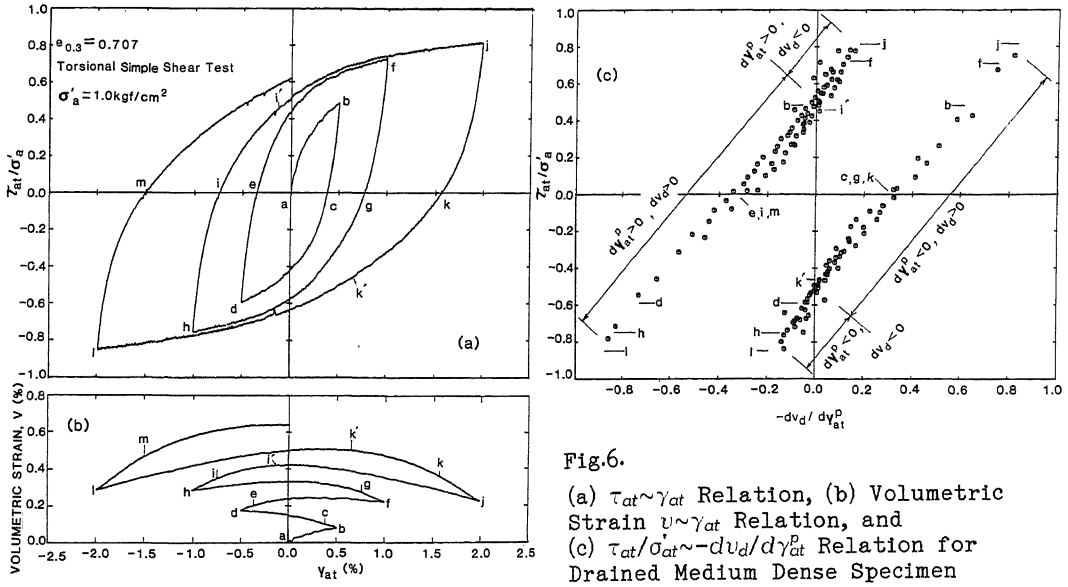

Fig.6.
(a) $\tau_{at}\sim\gamma_{at}$ Relation, (b) Volumetric Strain $v\sim\gamma_{at}$ Relation, and (c) $\tau_{at}/\sigma'_{at}\sim -dv_d/d\gamma^p_{at}$ Relation for Drained Medium Dense Specimen

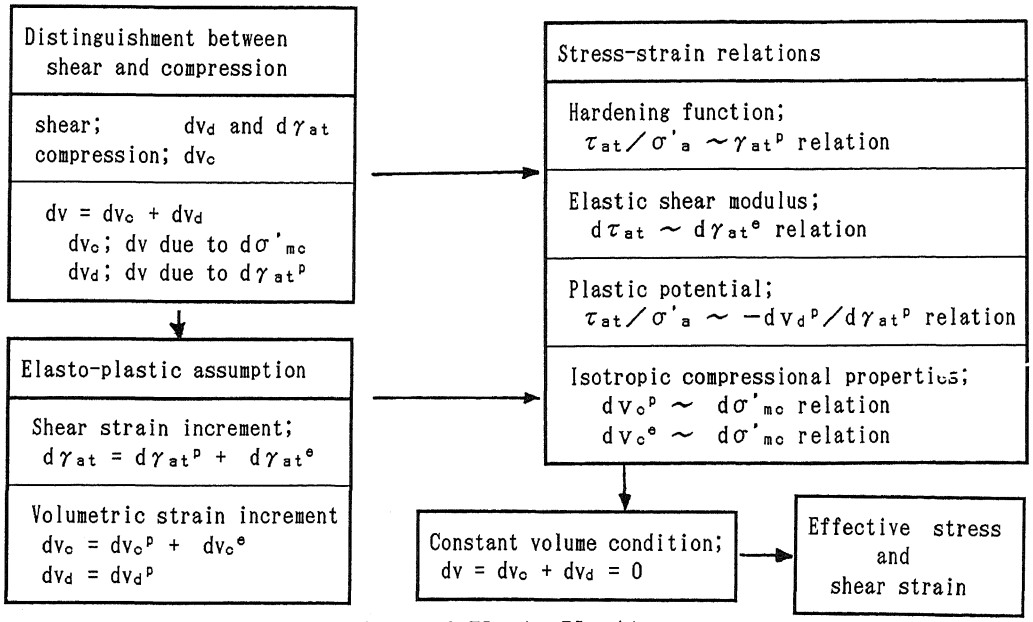

Fig.7. Structure of Elasto-Plastic Model for Liquefaction Analysis

$d\upsilon_d/|d\gamma^p_{at}|$) during unloading is larger during unloading from a larger τ_{at}/σ'_a (see Fig.6c). On the other hand, it may be noted that during unloading from a larger τ_{at}/σ'_a, for example from j to k, a larger absolute value of $d\gamma_{at}$ takes place (Fig.6a). It may also be noted that also for the initial portion of reloading from k, the shear strain increment has become larger than that during the first reloading from c. Consequently, from the above two reasons, the rate of volume decrease becomes larger after the loading direction is reversed from a larger τ_{at}/σ'_a as shown in Fig.6(b). This drained behavior is well in accordance with that in the undrained tests; i.e., the build-up of Δu during unloading and reloading becomes larger when unloaded from a larger τ_{at}/σ'_a above the phase transformation line.

(3) It may be seen from Figs 3(d) and 5(d) that at relatively large strains the direction of σ'_1-direction tends to be close to ±45 degrees from the σ'_a-direction. This is because at relatively large strains the directions of σ'_1 and the plastic major principal strain increment $d\varepsilon^p_1$ tend to coincide, and $d\varepsilon^p_1$ is nearly equal to the total major principal strain increment $d\varepsilon_1$, the directions of which are always at ±45° from the σ'_a-direction. This means that the effects of continuous rotation (not the discontinuous rotation between ±45°) on the vertical planes of $d\varepsilon^p_1$ and σ'_1 may not be significant in such cyclic undrained simple shear testing. However, the effects of continuous rotation on the horizontal planes of $d\varepsilon^p_1$ and σ'_1 due to multi-directional earthquake motions may be very important in the field during earthquake.

SUMMARY AND CONCLUSIONS

The results of the cyclic undrained simple shear tests presented in this paper provide a rationale for several elasto-plastic models based on strain-hardening hyperbolic relations between the stress ratio (τ_{at}/σ'_a) and the shear strain (γ_{at}), which have been proposed for simulating cyclic undrained behavior of liquefying sand. Furthermore, the change in σ'_a or Δu is to be related to the volume change as observed in cyclic drained tests, which is, in turn, related to the plastic shear strain increment through the stress-dilatancy relation. Based on these results, such a model as shown in Fig.7 can be suggested. In this model, the effects of continuous rotation of σ'_1 are ignored.

ACKNOWLEDGMENTS

The authors express their sincere thanks to Mr. T. Sato and Miss M. Torimitsu for their helps.

REFERENCES

1. Ishihara, K., Tatsuoka, F. and Yasuda, S., Undrained Deformation and Liquefaction of Sand under Cyclic Stresses, Soils and Foundations, 15-1, pp.29-44, 1975.
2. Tatsuoka, F., Some Recent Developments in Triaxial Testing Systems for Cohesionless Soils, ASTM, Advanced Triaxial Testing of Soil and Rock, STP 977, pp.7-67, 1988.
3. Pradhan, T.B.S., Tatsuoka, F. and Horii, N., Simple Shear Testing on Sand in a Torsional Shear Apparatus, Soils and Foundations, 28-2, pp.95-112, 1988.
4. Tatsuoka, F., Sonoda, S., Hara, K., Fukushima, S. and Pradhan, T.B.S., Failure and Deformation of Sand in Torsional Shear, Soils and Foundations, 26-4, pp.79-97, 1986.
5. Pradhan, T.B.S., Tatsuoka, F. and Sato, Y., Experimental Stress-Dilatancy Relations of Sand Subjected to Cyclic Loading, Soils and Foundations, 1988 (Submitted).